Astronomy & Astrophysics manuscript no. GRB111117A
2017-07-06
©ESO 2017

arXiv:1707.01452v1 [astro-ph.HE] 3 Jul 2017

The host galaxy of the short GRB 111117A at $z = 2.211$: impact on the short GRB redshift distribution and progenitor channels⋆

J. Selsing[1], T. Krühler[2], D. Malesani[1], P. D'Avanzo[3], S. Schulze[4,5,6], S. D. Vergani[3,7], J. Palmerio[8], J. Japelj[9], B. Milvang-Jensen[1], D. Watson[1], P. Jakobsson[10], J. Bolmer[2], Z. Cano[11], S. Covino[12], V. D'Elia[12,13], A. de Ugarte Postigo[11,1], J. P. U. Fynbo[1], A. Gomboc[14], K. E. Heintz[10,1], L. Kaper[9], A. J. Levan[15], S. Piranomonte[16], G. Pugliese[9], R. Sánchez-Ramírez[11,17], M. Sparre[1,18], N. R. Tanvir[19], C. C. Thöne[11], and K. Wiersema[19]

[1] Dark Cosmology Centre, Niels Bohr Institute, University of Copenhagen, Juliane Maries Vej 30, 2100 København Ø, Denmark
[2] Max-Planck-Institut für extraterrestrische Physik, Giessenbachstraße, 85748 Garching, Germany
[3] INAF - Osservatorio Astronomico di Brera, via E. Bianchi 46, I-23807, Merate (LC), Italy
[4] Instituto de Astrofísica, Facultad de Física, Pontificia Universidad Católica de Chile, Vicuña Mackenna 4860, 7820436 Macul, Santiago, Chile
[5] Millennium Institute of Astrophysics, Vicuña Mackenna 4860, 7820436 Macul, Santiago, Chile
[6] Department of Particle Physics and Astrophysics, Faculty of Physics, Weizmann Institute of Science, Rehovot 76100, Israel
[7] GEPI, Observatoire de Paris, PSL Research University, CNRS, Place Jules Janssen, 92190 Meudon, France
[8] Sorbonne Universités, UPMC Univ. Paris 6 et CNRS, UMR 7095, Institut d'Astrophysique de Paris, 98 bis bd Arago, 75014 Paris, France
[9] Anton Pannekoek Institute for Astronomy, University of Amsterdam, Science Park 904, 1098 XH Amsterdam, The Netherlands
[10] Centre for Astrophysics and Cosmology, Science Institute, University of Iceland, Dunhagi 5, 107 Reykjavík, Iceland
[11] Instituto de Astrofísica de Andalucía (IAA-CSIC), Glorieta de la Astronomía s/n, E-18008, Granada, Spain
[12] INAF-Osservatorio Astronomico di Roma, Via Frascati 33, I-00040 Monteporzio Catone, Italy
[13] ASI-Science Data Centre, Via del Politecnico snc, I-00133 Rome, Italy
[14] Centre for Astrophysics and Cosmology, University of Nova Gorica, Vipavska 13, 5000 Nova Gorica, Slovenia.
[15] Department of Physics, University of Warwick, Coventry CV4 7AL, UK
[16] INAF, Osservatorio Astronomico di Brera, Via E. Bianchi 46, I-23807 Merate (LC), Italy
[17] Istituto de Astrofisica e Planetologia Spaziali, INAF, Via Fosso del Cavaliere 100, I-00133 Roma, Italy
[18] Heidelberger Institut für Theoretische Studien, Schloss-Wolfsbrunnenweg 35, 69118 Heidelberg, Germany
[19] Department of Physics & Astronomy and Leicester Institute of Space & Earth Observation, University of Leicester, University Road, Leicester, LE1 7RH, UK

Received/ accepted

ABSTRACT

It is notoriously difficult to localize short γ-ray bursts (sGRBs) and their hosts to measure their redshifts. These measurements, however, are critical to constrain the nature of sGRB progenitors, their redshift distribution and the r-process element enrichment history of the universe. Here, we present spectroscopy of the host galaxy of GRB 111117A and measure its redshift to be $z = 2.211$. This makes GRB 111117A the most distant high-confidence short duration GRB detected to date. Our spectroscopic redshift supersedes a lower, previously estimated photometric redshift value for this burst.

We use the spectroscopic redshift, as well as new imaging data to constrain the nature of the host galaxy and the physical parameters of the GRB. The rest-frame X-ray derived hydrogen column density, for example, is the highest compared to a complete sample of sGRBs and seems to follow the evolution with redshift as traced by the hosts of long GRBs (lGRBs).

The host lies in the brighter end of the expected sGRB host brightness distribution at $z = 2.211$, and is actively forming stars. Using the host as a benchmark for redshift determination, we find that between 43 and 71 per cent of all sGRB redshifts should be missed due to host faintness for hosts at $z \sim 2$. The high redshift of GRB 111117A is evidence against a lognormal delay-time model for sGRBs through the predicted redshift distribution of sGRBs, which is very sensitive to high-z sGRBs.

From the age of the universe at the time of GRB explosion, an initial neutron star (NS) separation of $a_0 < 3.2\ R_\odot$ is required in the case where the progenitor system is a circular pair of inspiralling NSs. This constraint excludes some of the longest sGRB formation channels for this burst.

Key words. gamma-ray burst: individual: GRB 111117A – gamma-ray burst: general – galaxies: high-redshift – binaries: general – X-rays: bursts – techniques: imaging spectroscopy

1. Introduction

There is mounting evidence that short-duration γ-ray bursts come from the merger of NSs, either with another NS, or a black hole, due to their apparent association with kilonovae (Barnes & Kasen 2013, Tanvir et al. 2013, Yang et al. 2015, Jin et al.

⋆ Based on observations collected at ESO/VLT under programme 088.A-0051 and 091.D-0904, at TNG under programme A24TAC_38, at Gemini North under programme GN-2011B-Q-10 and GTC under programme GTC43-11B.

2016, Rosswog et al. 2017). The absence of associated supernovae in deep searches (e.g. Hjorth et al. 2005a, Fox et al. 2005, Hjorth et al. 2005b, Kann et al. 2011) supports this idea and distinguishes the physical origin of sGRBs from their long-duration counterparts, (albeit see also Fynbo et al. 2006, Della Valle et al. 2006, Gal-Yam et al. 2006).

The classification of GRBs in two groups, initially comes from the bimodal distribution of burst duration and spectral hardness (Kouveliotou et al. 1993), where the duration $T_{90} < 2$ has been regarded as the dividing line between long and short GRBs. Additionally, it has been found for lGRBs that there is a spectral lag in the arrival-time of photons, with the most energetic ones arriving first. This lag is consistent with zero for sGRBs (Norris & Bonnell 2006). Because both populations have continuous, overlapping distributions in their observables and because telescopes observe in differing bands, it is difficult to impose a single demarcation criterion between the two classes. For this reason, the distinction between long and short GRBs is preferably based on a combination of high-energy properties (Zhang et al. 2009, Bromberg et al. 2012, 2013).

The *Swift* satellite (Gehrels et al. 2004) greatly improved the understanding of sGRB progenitors thanks to its quick localization capability. The bulk of these localizations have associated galaxies at relatively low redshifts with a median redshift of $z \sim 0.5$ (Berger 2014), and because most of these measurements come from the associated hosts, it is arguably biased towards lower redshifts. The host galaxies of sGRBs are diverse. They are more massive and less actively star-forming on average than lGRB hosts (Fong et al. 2013), while in some cases, no host galaxy can be identified above detection threshold of deep follow-up observations (Berger 2010, Tunnicliffe et al. 2014). Together with their position within their hosts (Fong & Berger 2013), this suggests a progenitor system that can be very long lived in comparison to lGRBs, and is tracing with host stellar mass rather than star-formation rate (SFR).

The electromagnetic signals from sGRBs are a promising channel to accurately localize NS mergers, which holds the promise for a detection of an associated gravitational wave (GW) signal (Ghirlanda et al. 2016). The simultaneous detection of a sGRB and a GW will provide new promising ways to constrain the binary inclination angle (Arun et al. 2014) and measure cosmological distances (Nissanke et al. 2010).

The total lifetimes of NS binaries depends on their orbit, mass, spin, initial separations and subsequent inspiral times. The delay time from formation to explosion impacts the timing and distribution of the enrichment of the ISM with heavy *r*-process elements (van de Voort et al. 2014, Wallner et al. 2015, Ji et al. 2016). Some limits can be calculated using host galaxy star-formation history models and spatial distribution of sGRBs within their hosts (Berger 2014). The most distant cosmological bursts, however, offer direct, hard limits on the coalescence time scales.

We here present a spectrum of the host galaxy of the short GRB 111117A ($T_{90} = 0.46$ s) and measure its redshift to be $z = 2.211$. This value is significantly higher than the previously estimated redshift based on photometric studies (Margutti et al. 2012, Sakamoto et al. 2013). We present the GRB's rest frame properties based on this new distance compared to previous analyses and revisit the host properties derived from the new solution to the spectral energy distribution (SED) fit. While no optical afterglow was detected, the excellent localization from a detection of the X-ray afterglow by the *Chandra X-ray Observatory* allows us to discuss the positioning and environmental properties of this remarkably distant sGRB. We use the ΛCDM cosmology parameters provided by Planck Collaboration et al. (2016) in which the universe is flat with $H_0 = 67.7\,\mathrm{km\,s^{-1}}$ and $\Omega_m = 0.307$. All magnitudes are given in the AB system.

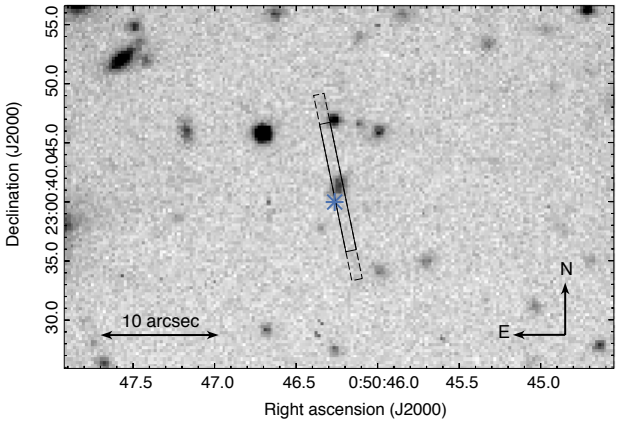

Fig. 1. FORS2 R-band imaging of the field of GRB 111117A with the X-shooter slit overlaid. The slit position represents 4 epochs of spectroscopic observations taken at similar position angles. The corresponding photometry is shown in Fig. 3. The blue asterisk indicates the GRB position as derived from the *Chandra* observations in Sakamoto et al. (2013).

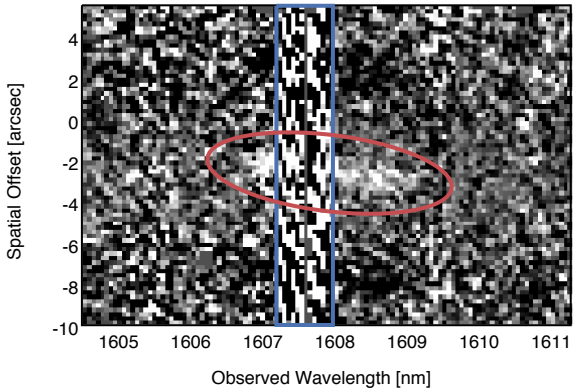

Fig. 2. 2D-image of the [O III]λ5007 emission line. The location of a bright skyline is marked by the blue box. The location of the emission line is indicated with the red ellipse. Because the host is observed in nodding-mode, negative images of the emission line appear on both sides in the spatial direction.

2. Observations and results

2.1. Spectroscopic observations and analysis

Spectroscopic observations were carried out using the cross-dispersed echelle spectrograph, VLT/X-shooter (Vernet et al. 2011), at four seperate epochs. The burst was observed 38 hours after the Burst Alert Telescope (BAT) trigger under ESO programme 088.A-0051 (PI: Fynbo) and again later under ESO programme 091.D-0904 (PI: Hjorth). Observations use a simple ABBA nodding pattern, using 5 arcsec nod throws. X-shooter covers the wavelength range from 3000 Å to 24 800 Å (21 000 Å when the *K*-band blocking filter is used) across three spectroscopic arms. We carried out the bias-correction, flat-fielding, order tracing, wavelength calibration, rectification, and flux calibration using the VLT/X-shooter pipeline version 2.8.4 (Goldoni et al. 2006, Modigliani et al. 2010) run in physical mode. Because the echelle or-

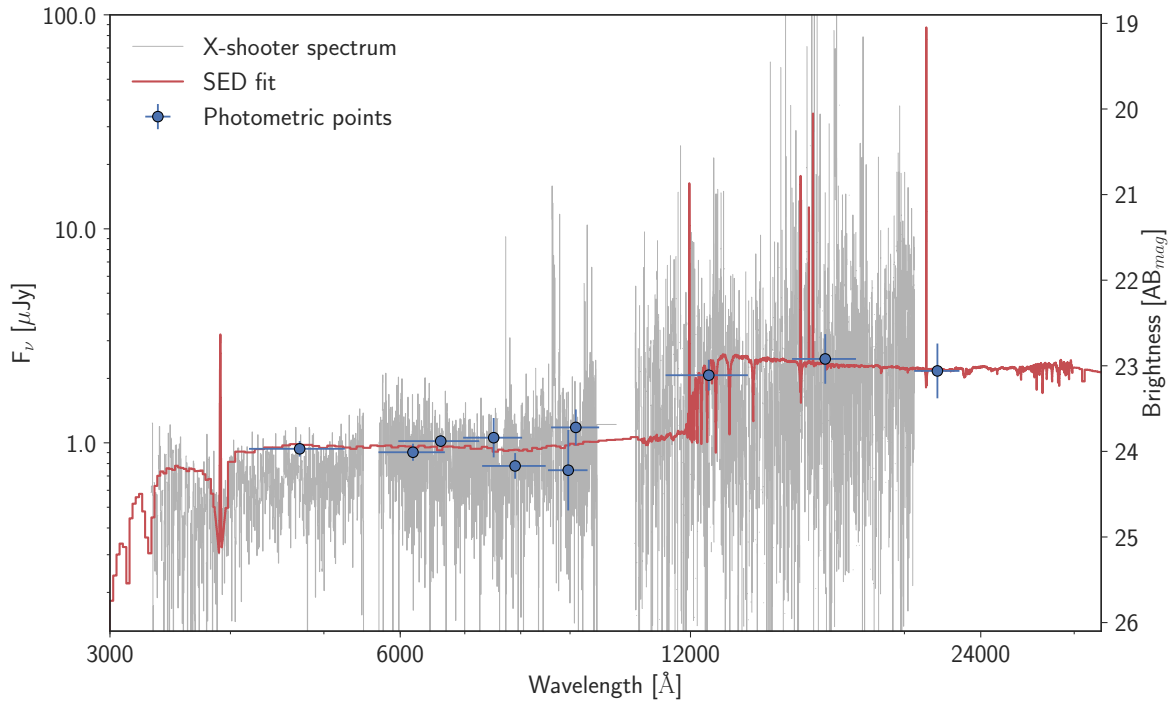

Fig. 3. SED fit showning the best-fist SED to the derived photometry. The detection of Lyα is predicted from the SED fit and confirmed by the spectroscopic observations. Overplotted in grey is the observed spectrum, binned down to 3 Å per pixel for presentation purposes. Slit losses are responsible for discrepancies between the measured photometry and the X-shooter spectrum. The reason for the spectral gaps at 5500 Å and 10000 Å is from the merging of the arms.

ders are curved across each detector, a rectification algorithm is employed which introduces correlations between neighboring pixels. We select a pixel-scale of 0.2/0.2/0.6 Å/pix for the UVB/VIS/NIR arm to minimize the degree of correlation while conserving the maximal resolution. The observations are combined and extracted using scripts described in Selsing et al. 2017 (in prep.) and available online[1], where the full spectral point spread function is modeled across each arm and used for the optimal extraction algorithm (Horne 1986). An overview of the spectroscopic observations is given in Table 1, and the slit position is shown in Fig. 1. We show the extracted spectrum in Fig. 3.

We determine a redshift of $z = 2.211$ from the simultaneous detection of emission lines belonging to Lyα, [O II]λ3727, Hβ, [O III]λ5007, and Hα. Hβ is detected at low significance ($\sim 3\sigma$). We show [O III]λ5007 in the insert in Fig. 2. Hα is only visible in the first epoch due to the K-band blocking filter used for the remaining observations. The nebular lines exhibit a spatial extent of $\sim 1\farcs5$ and show significant velocity structure along the slit. A drop in the continuum bluewards of the Lyα line further supports the inferred redshift.

Using the luminosity of Hα, we can infer the star-formation rate (SFR) of the host (Kennicutt 1998). At the redshift of the GRB host, Hα is observed at 21 000 Å where the night sky is very bright. In addition, several bright sky-lines are superposed on the line, making an accurate estimate of the Hα-flux difficult. We obtain a limit on the SFR by numerically integrating the part of Hα free of contamination and correcting for the missing flux using the line profile and obtain $F_{H\alpha} > 4.1 \times 10^{-17}$ergs^{-1}cm^{-2}. After converting the Kennicutt (1998) relation to a Chabrier (2003) initial mass function using Madau & Dickinson (2014), we derive a limit of $SFR > 7 M_\odot$ yr^{-1}. Additionally, based on the width of [O III], an aperture covering the line is integrated over, where synthetic sky lines (Noll et al. 2012, Jones et al. 2013) have been masked and interpolated over. From the integrated Hα-line, we estimate SFR = 18 ± 3 M$_\odot$ yr^{-1}. From the SED-fit (Sect. 2.2), and the detection of Lyα, the host is constrained to contain very little or no dust, although the presence of Lya does not exclude dust. Therefore we do not apply a dust-correction to the measured Hα flux here. [O II] is close to a region of strong telluric absorption, which is why no SFR is inferred from this line.

The total extent of the lines in velocity space is $\sim$ 450 km/s. The line profiles shows an asymmetric "double-horned" profile, indicating that we are seeing a galaxy with a large degree of coherent rotational motion relative to the line-of-sight. If we assume that we are viewing a spiral galaxy edge-on, this is a measure of the rotational velocity of the gas. If we assume that the spectral resolution and the turbulent width of the lines are negligible compared to the rotational velocity, we can, based on the projected size of the source and the width of the lines, put a constraint on the dynamical mass of the galaxy (de Blok & Walter 2014). Based on the physical size along the slit and the velocity width of [O III]λ5007, we infer $M_{dyn} \gtrsim 10^{10.8}$ M$_\odot$. Because we are viewing the host inclined at an angle relative to edge-on and because the slit is not aligned along the long axis of the host, this value is a lower limit.

2.2. Imaging observations and SED analysis

In addition to the spectroscopy presented above, we imaged the field of GRB 111117A in multiple broad-band filters using the VLT equipped with FORS2 ($gRIz$ filters) and HAWK-I (JHK_s

[1] https://github.com/jselsing/XSGRB_reduction_scripts

Table 1. Overview of the spectroscopic observations. JH in the slit width refers to observations where a K-band blocking filter has been used. The seeing is determined from the width of the spectral trace of a telluric standard star, taken close in time to the host observation. The spectral resolution, R, is measured from unresolved telluric absorption lines in the spectrum of the telluric standard star.

Obs. Date	Exposure time (s)			Slit width	Airmass	Seeing	R
	UVB	VIS	NIR	(arcsec)		(arcsec)	VIS/NIR
2011-11-19T01:33	2×2400	2×2400	8×600	1.0/1.0/0.9	1.49	0.75	11600/6700
2013-07-15T09:02	2×1200	2×1200	8×300	1.0/1.0/0.9JH	1.53	0.98	9600/8900
2013-08-03T07:37	2×1200	2×1200	8×300	1.0/1.0/0.9JH	1.55	0.85	11400/11300
2013-08-03T08:34	2×1200	2×1200	8×300	1.0/1.0/0.9JH	1.49	0.85	11400/11300

filters), long after the burst faded. These new data are complemented by a re-analysis of some of the imaging used in Margutti et al. (2012) and Sakamoto et al. (2013) that are available to us (GTC *gri*-band, TNG *R*-band, and Gemini *z*-band). A log of the photometric observations and measured brightnesses is given in Table 2. Due to the optical darkness of this burst, see Sect. 2.3, there is likely no afterglow contamination on the measured photometry.

All data were reduced, analyzed and fitted in a similar manner as described in detail in Krühler et al. (2011) and, more recently, in Schulze et al. (2016). Briefly, we use our own `Python` and IRAF routines to perform a standard reduction which includes bias/flat-field correction, de-fringing (if necessary), sky-subtraction, and stacking of individual images. The photometry of the host was calibrated relative to field stars from the SDSS and 2MASS catalogs in the case of $grizJHK_s$ filters. For the *R* and *I*-band photometry, we used the color transformations of Lupton[2]. We convert all magnitudes into the AB system, and correct for a Galactic foreground of $E_{B-V} = 0.027$ mag (Schlegel et al. 1998, Schlafly & Finkbeiner 2011).

The multi-color SED is fit using the Bruzual & Charlot (2003) single stellar population models based on a Chabrier (2003) with initial mass function in *LePhare* (Ilbert et al. 2006), where the redshift is fixed to the spectroscopic value of $z = 2.211$. The best fit model is an unreddened galaxy template, and returns physical parameters of absolute magnitude ($M_B = -22.0 \pm 0.1$ mag), stellar mass ($\log(M_\star/M_\odot) = 9.9 \pm 0.2$), stellar population age ($\tau = 0.5^{+0.5}_{-0.3}$ Gyr) and star-formation rate ($SFR_{\rm SED} = 11^{+9}_{-4} M_\odot\,{\rm yr}^{-1}$). We show the SED fit in Fig. 3.

Noteworthy is the discrepancy of our new VLT/FORS2 photometry and the re-analysis of the Gemini data to the *z*-band measurements of Margutti et al. (2012) and Sakamoto et al. (2013). Both of these authors report *z*-band photometry that is brighter by 0.8 mag to 1.0 mag compared to our value, where data taken in bluer filters are in excellent agreement. The large $i - z$ color was mistakenly interpreted as a 4000 Å break driving the galaxy photometric redshift of the earlier works. Using the revised photometry from Table 2, the photometric redshift of the galaxy is $z_{\rm phot} = 2.04^{+0.19}_{-0.21}$, consistent with the spectroscopic value at the $1\,\sigma$ confidence level.

2.3. X-ray temporal and spectral analysis

We retrieved the automated data products provided by the *Swift*-XRT GRB repository[3] (Evans et al. 2009). The X-ray afterglow light curve can be fit with a single power-law decay with an index $\alpha = 1.27^{+0.12}_{-0.10}$. We performed a time-integrated spectral analysis using data obtained in photon counting (PC) mode in the widest time epoch where the $0.3-1.5$ keV to $1.5-10$ keV hardness ratio is constant (namely, from $t - T_0 = 205$ s to $t - T_0 = 203.5$ ks, for a total of 29.1 ks of data) to prevent spectral changes that can affect the X-ray column density determination (Kopač et al. 2012). The obtained spectrum is well described by an absorbed power-law model and the best-fit spectral parameters are a photon index of 2.1 ± 0.4 and an intrinsic equivalent hydrogen column density $N_{\rm H}$ of $2.4^{+2.4}_{-1.6} \times 10^{22}$ cm^{-2} ($z = 2.211$), assuming a solar abundance and a Galactic $N_{\rm H}$ in the burst direction of 4.1×10^{20} cm^{-2} (Willingale et al. 2013).

A measure of the optical-to-X-ray flux ratio is parametrized in terms of the "darkness"-parameter β_{OX} (Jakobsson et al. 2004). Using the optical afterglow limits (Cucchiara & Cenko 2011, Cenko & Cucchiara 2011), the X-ray lightcurve can be interpolated and evaluated at the time of the non-detection. We find $\beta_{OX} < 0.79$, consistent with what was reported in Sakamoto et al. (2013).

3. Reinterpretation of the restframe properties

Because the projected distance does not change significantly between $z = 1.3$ and $z = 2.211$, all conclusions of Margutti et al. (2012) and Sakamoto et al. (2013) relating to host offset are unaffected.

3.1. Classification

As pointed out by Margutti et al. (2012) and Sakamoto et al. (2013), GRB 111117A is securely classified as a sGRB. Because the observed classification indicators, T_{90} and hardness ratio, do not depend strongly on redshift (Littlejohns et al. 2013), the updated redshift does not change this designation. The intrinsic spectral lag shortens, but since it is already consistent with zero, this does not affect the classification.

The intrinsic luminosity is shown in the X-ray light curve (Fig. 4) and it is sub-luminous compared to the majority of long GRBs. The inset in Fig. 4 shows the luminosity distribution at 10 ks. The sub-samples comprise of 333 long, 19 short GRBs, and GRB 111117A. The mean and the 1-σ dispersions of the samples are $L_{lGRB} = 46.59 \pm 0.87$ and $L_{sGRB} = 44.96 \pm 0.94$. GRB 111117A had a luminosity of 44.95 at 10 ks which is very close to the peak of the sGRB luminosity distribution at 10 ks, but an outlier from the lGRG distribution, further supporting the short classification.

Bromberg et al. (2013) investigated the degree to which the long and short population distributions overlap and quantified the certainty in class membership. According to Bromberg et al. (2013), GRB 111117A has 96^{+3}_{-5} percent probability of being a sGRB. Compared to the other two sGRB candidates at high redshift, GRB 060121 (de Ugarte Postigo et al. 2006, Levan et al. 2006) at $1.7 \lesssim z \lesssim 4.5$ (17^{+14}_{-15} per cent) and GRB 090426 (An-

[2] https://www.sdss3.org/dr8/algorithms/sdssUBVRITransform.php
[3] http://www.swift.ac.uk/xrt_products/00507901

Table 2. Overview of the photometric observations.

Obs. Date	Exptime	Telescope/Instrument	Filter	Airmass	Image Quality	Host Brightness[a]
	ks				(arcsec)	($\mathrm{mag_{AB}}$)
2013-08-30T07:43	1.45	VLT/FORS2	g	1.55	0.99	24.08 ± 0.09
2011-11-17T20:07	0.80	GTC/OSIRIS	g	1.15	1.67	24.13 ± 0.09
2011-11-17T20:07	1.20	GTC/OSIRIS	r	1.11	1.50	23.93 ± 0.08
2013-07-17T08:37	1.45	VLT/FORS2	R	1.56	0.74	23.95 ± 0.06
2011-11-28T21:10	3.60	TNG/DOLORES	R	1.01	1.08	23.96 ± 0.13
2011-11-17T20:07	0.36	GTC/OSIRIS	i	1.08	1.50	23.89 ± 0.23
2013-08-03T09:23	1.35	VLT/FORS2	I	1.54	0.93	24.22 ± 0.15
2011-11-28T06:14	1.80	Gemini/GMOS-N	z	1.01	0.84	24.24 ± 0.47
2013-07-13T09:33	1.08	VLT/FORS2	z	1.49	0.63	23.76 ± 0.21
2013-06-24T09:14	1.98	VLT/HAWK-I	J	1.70	0.63	23.13 ± 0.18
2013-06-27T09:21	1.68	VLT/HAWK-I	H	1.63	0.91	22.94 ± 0.29
2013-06-28T09:14	1.92	VLT/HAWK-I	K_s	1.65	0.76	23.07 ± 0.32

Notes. [(a)] All magnitudes are given in the AB system and are not corrected for the expected Galactic foreground extinction corresponding to a reddening of $E_{B-V} = 0.027$ mag.

tonelli et al. 2009, Levesque et al. 2010, Thöne et al. 2011) at $z = 2.609$ (10^{+15}_{-10} per cent), the certainty in class membership for GRB 111117A is much higher.

Additionally, Horváth et al. (2010) classifies both GRB 060121 and GRB 090426 as intermediate duration bursts. This comes from both events having very soft spectra, as compared to the hard ones typically seen in sGRBs. Intermediate bursts are very clearly related in their properties to lGRBs (de Ugarte Postigo et al. 2011), so they are unlikely to come from compact object mergers.

The redshift and secure classification of GRB 111117A mean that it occurred when the universe was younger by 1.8 Gyr compared to any other non-collapsar GRB ever detected. This number is 3.2 Gyr for the next-highest spectroscopic redshift. If the merger of NSs is the primary agent for the r-process element enrichment of the universe (Goriely et al. 2011, Ji et al. 2016, Komiya & Shigeyama 2016), this marks the earliest detection of this process.

3.2. Restframe $N_{\rm H}$

We show the recalculated $N_{\rm H}$ in Fig. 5 where we compare with the distributions of complete samples of both long and short GRBs. The lGRB sample is from Arcodia et al. (2016) and the sGRB sample is from D'Avanzo et al. (2014). From the sGRB sample of D'Avanzo et al. (2014) we have excluded GRB 090426 which does likely not belong in a short sample as highlighted in Sect. 3.1. Both comparison samples consider the largest temporal interval of constant hardness ratio to prevent spectral changes that can affect the X-ray derived column density. The 17 (5) of the 99 (15) long (short) GRBs which do not have redshift have been excluded from our analysis.

GRB 111117A occupies a unique position in Fig. 5 with the highest N_H and highest redshift of all sGRBs. The short sample, excluding GRB 111117A, is located at low redshifts ($z < 1$) and is found to populate a column density environment similar to that of lGRBs at comparable redshifts (D'Avanzo et al. 2014). The inferred hydrogen column density for GRB 111117A seems to follow the trend with increasing N_H as a function of redshift as found for the lGRB afterglows (Campana et al. 2010, Starling et al. 2013, Arcodia et al. 2016). This is related to what is found by Kopač et al. (2012), Margutti et al. (2013), that N_H seems

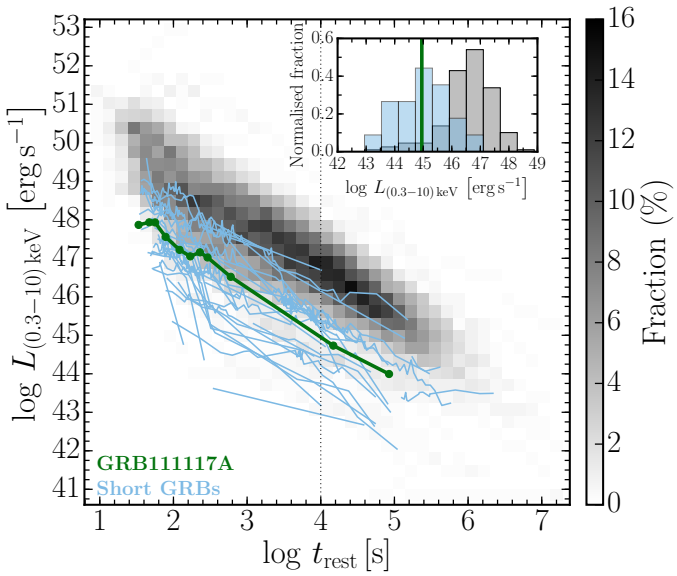

Fig. 4. Restframe XRT lightcurve of GRB 111117A, compared to the general population of XRT lightcurves of GRBs. The grey shaded region is a compilation of long GRB lightcurves (Evans et al. 2007, 2009) where the color represents density. The light blue lines are sGRB lightcurves from bursts with duration of $T_{90} \lesssim 2$ s and those that were classified as short in Kann et al. (2011), Berger (2014), D'Avanzo et al. (2014). The thick green line is GRB 111117A. Despite the remarkably high redshift, the luminosity is comparable to the bulk of the short burst population and subluminous compared to the lGRB population.

to be comparable for long and short GRBs when compared at similar redshifts.

The redshift evolution of N_H in the hosts of lGRBs is not reproduced by Buchner et al. (2017), using a different N_H inference methodology. Instead a correlation between N_H and host stellar mass is suggested. Assuming that the different N_H-fitting methodologies yield comparable results, GRB 111117A is an outlier from the relation suggested by Buchner et al. (2017) by more than the intrinsic scatter, although some lGRB hosts populate a similar region in the N_H-$M_\star$ relation. Additionally, for lGRBs, N_H correlates with the surface luminosity at the explosion site (Lyman et al. 2017). The large offset of GRB 111117A

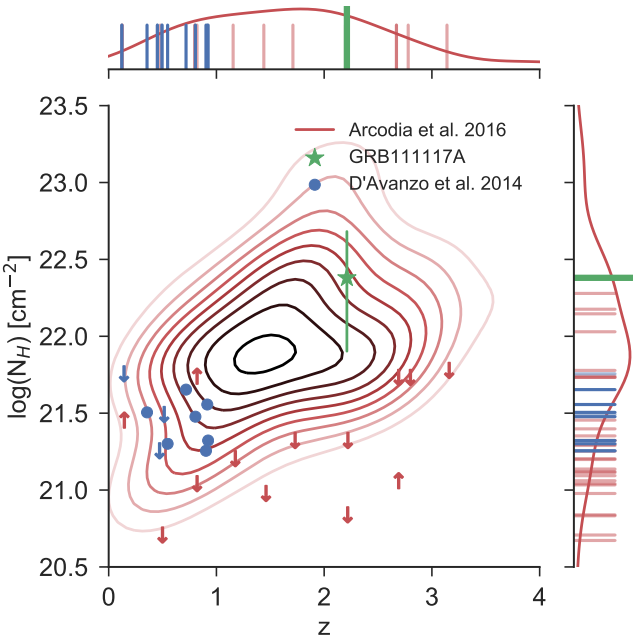

Fig. 5. Rest frame, X-ray derived equivalent hydrogen column densities for GRB 111117A compared to complete samples of both long and short populations of GRBs. The detections are replaced with contours and the limits are shown with arrows. Marginalizations over both axes are shown where the limits are shown as transparent bars and detections as solid ones.

relative to the host center derived in Margutti et al. (2012) and Sakamoto et al. (2013) is difficult to reconcile with galaxy-scale gas providing the X-ray absorption. Along with the absence of dust, the large offset from the host center indicates that the high N_H arises because the density in the GRB surrounding is high, or because the light from the afterglow traverses a region of dense gas. The optical darkness of the GRB is an additional hint of the high density in the GRB surroundings or along the line of sight.

3.3. Host galaxy

From the clear host association, GRB 111117A does not belong to the hostless class of GRBs (Berger 2010) and because the host exhibits emission lines this is indicative of a population of relatively young stars. As the majority of sGRBs (Fong et al. 2013), the host of GRB 111117A is therefore a late-type galaxy and is entirely consistent in terms of stellar mass and stellar age with the general population of sGRB hosts ($\langle M_* \rangle = 10^{10.1} M_\odot$ and $\langle \tau_* \rangle = 0.3$ Gyr) (Leibler & Berger 2010). Being a late-type host, both the stellar mass and sSFR are entirely within the range expected for the hosts of sGRBs (Behroozi et al. 2014). Our constraints on the dynamical mass is also well accommodated by the expected sGRB host halo mass (Behroozi et al. 2014).

The SFR is ∼1 order of magnitude higher than the typical SFR for sGRB host galaxies (Berger 2014) and more similar to the SFR found in the hosts of lGRBs at a corresponding redshift (Krühler et al. 2015). Only two hosts in the sample of short GRBs compiled in Berger (2014) have a more vigorous star formation, meaning that it is in the very upper end of the star formation distribution. The cosmic SFR evolution of the universe likely plays a role due to the proximity of GRB 111117A to the peak of cosmic SFR (Madau & Dickinson 2014). The high SFR is partly a selection effect, because a less star forming galaxy would exhibit weaker emission lines, thus making the redshift harder to determine. Additionally, it is natural to expect some evolution in the hosts of sGRBs with redshift as illustrated for N_H in Sect. 3.2.

The detection of Lyα is consistent with the SED-inferred absence of dust, despite the moderate stellar age which would suggest the opposite. The centroid of the Lyα emission is found to be redshifted by ~ 220 km s^{-1} with respect to systemic, which is similar to what is found for long GRB hosts (Milvang-Jensen et al. 2012) where the outflow is attributed to star formation.

4. Implications for the redshift distribution of sGRBs

A single sGRB at high redshift does little in terms of constraining the redshift distribution of sGRBs. In particular, other sGRB hosts could be missed because they are intrinsically fainter and thus the high redshift of GRB 111117A is only measured due to the brightness of its host. Berger (2014) compiled a sample of sGRB host luminosities, normalized by the characteristic galaxy luminosity at their respective redshift, $L_B/L_B^\star$. To convert the SED-inferred M_B of GRB 111117A to $L_B/L_B^\star$, we use the characteristic absolute B-band magnitude of the Schechter function for blue galaxies ($U-V < 0.25$) in the redshift window $2.0 \leq z \leq 2.5$ from Marchesini et al. (2007) and obtain $L_B/L_B^\star = 1.2$.

Using the complete, flux-limited selection of bursts from D'Avanzo et al. (2014), excluding GRB 111117A and the likely non-sGRB GRB 090426, we have a statistically homogeneous sample from which we can address the implications of the redshift of GRB 111117A. Out of the 14 hosts in the sample, 10 (71 per cent) have measured redshifts and $L_B/L_B^\star$. Of the complete sample, the host of GRB 111117A is brighter than 80 per cent of the hosts with measured $L_B/L_B^\star$. Even if we conservatively assume that *all* the hosts missing $L_B/L_B^\star$ are brighter than the host of GRB 111117A, the host is still brighter than > 60 per cent of sGRB hosts. For all 26 hosts with $L_B/L_B^\star$ from Berger (2014), the host of GRB 111117A is brighter than 73 per cent.

If we assume that we are able to obtain emission-line redshifts from hosts, 0.5 mags fainter ($R < 24.5$ mag; Krühler et al. 2012), then we would have missed 60 per cent of the redshifts (6 out of 10 hosts), due too the host being too faint, were they at the redshift of GRB 11117A. The corresponding number is around 45 per cent (12 out of 26) from the full sample of Berger (2014), reflecting the lower mean $L_B/L_B^\star$ of the complete sample. Because the average SFR of galaxies hosting lGRBs is higher than for galaxies hosting sGRBs, the fraction of missed burst redshifts is likely higher although the cosmic SFR evolution could play a role in improving redshift determinability.

A fraction of the bursts missing redshift are host-less but appear to be spatially correlated with galaxies that are likely at moderate redshifts (Tunnicliffe et al. 2014), but should some of the remainder be at high redshift, the missed fraction will increase. If we assume that *all* the bursts that are missing redshifts are at high-z and missed due to host faintness, 10 out of 14 hosts in the complete sample (71 per cent) would be missed at $z = 2.211$. This serves as an upper limit on the fraction of missed burst redshifts at high-z. Conversely, if all bursts missing redshift are at low redshift and missed for other reasons, 6 out of 14 hosts (43 per cent) would be missed at $z = 2.211$. The two limits indicate that we would miss between 43 and 71 per cent of sGRB hosts at $z \sim 2$ due to host faintness.

The theoretical redshift distribution of sGRBs depends on the type of delay-time function used to model the progenitor

system. The likelihood preferred lognormal time delay models investigated by Wanderman & Piran (2015) predict a sGRB rate at $z = 2.211$, $\sim$ two orders of magnitude lower compared to the peak rate at $z = 0.9$. According to Wanderman & Piran (2015), this preference depends critically on the absence of non-collapsar sGRBs at $z \gtrsim 1.2$. The higher determined redshift of GRB 111117A, and the likely number of additional high-z sGRB could change the preferred time delay models. The redshift of GRB 111117A, on the other hand, is close to the expected peak in sGRB rate calculated using the power law delay time models (Behroozi et al. 2014, Wanderman & Piran 2015, Ghirlanda et al. 2016), meaning we could be missing a large fraction of sGRBs.

5. Constraints on progenitor separation

At $z = 2.211$, the age of the universe is 3 Gyr. If the progenitor systems of sGRBs are the merger of two NSs, this sets a hard upper limit to the coalescence timescale for such a system. In the absence of other mechanisms, the timescale of the orbital decay of the system is set by the energy loss due to gravitational waves, which in turn is set by the mass of the constituent compact objects, the eccentricity of the orbit and the separation of the two (Postnov & Yungelson 2014). If we assume that the formation timescale of the first galaxies is short compared to the time since the Big Bang (Richard et al. 2011), and if we assume a mass of 1.4 $M_{\odot}$ for each of the NSs in a circular orbit at the time of system formation, this places a hard upper limit on the initial separation, of $a_0 < 3.2\ R_{\odot}$.

In practice most NS-NS binaries will be eccentric at formation because of the SN natal kicks. For more eccentric orbits, the coalescence timescale decreases, leading to a decrease in the constraint on the initial separation and larger initial separation constraints. As noted by Postnov & Yungelson (2014), it takes eccentricities > 0.6 to significantly shorten the merger time.

Using the inferred stellar population age from our SED fit, then we obtain a (softer) limit on the initial separation of $a_0 < 2.1\ R_{\odot}$. However, this does not account for the possibility there could be an underlying stellar population of older stars from a previous star-formation epoch. To investigate the possible impact of the presence of an old stellar population, we followed Papovich et al. (2001) and re-fitted the observed SED with the best-fit template to which an additional stellar population of old stars was added. For each galaxy, this old population was set as the SPSs with same parameters that the best-fit SED excepts the age, which was set to the age of the Universe at the observed redshift. In principle, this can constrain the maximum contribution of old populations within the photometric error bars (see Papovich et al. 2001, for details). We find a negligible contribution to the stellar mass (i.e. variations much smaller than the statistical uncertainty associated with the best-fit template). The delay time between formation and explosion is well accommodated by the models of Belczynski et al. (2006), although the longest delay times are excluded. This is especially true given the late type nature of the host (O'Shaughnessy et al. 2008).

6. Conclusions

We have here provided a revised, spectroscopic redshift measurement for the short GRB 111117A based on host galaxy emission lines setting it at $z = 2.211$. This value supersedes the previous photometric redshift of Margutti et al. (2012) and Sakamoto et al. (2013). The erroneous redshift estimate of previous authors is attributed to a discrepancy in the measured z-band magnitude, and highlights the importance of deep spectroscopic studies of sGRB hosts at medium resolution.

Using the new distance, the X-ray derived N_H towards GRB 111117A is the highest within a complete sample of sGRB hosts and is consistent with the $N_H - z$ evolution traced by the hosts of lGRBs. The SFR of the host is in the upper end of the sGRB host SFR distribution and no significant amount of dust is present. The high N_H is difficult to reconcile with the large projected host offset and the absence of dust. One possible explanation could be, that GRB 111117A is formed through a prompt channel of sGRB formation and originates in a star forming region located in the outskirts of the host.

Although a single burst carries little leverage in terms of constraining the redshift distribution of sGRB, the high redshift of GRB 111117A needs to be accommodated in progenitor models. A lognormal delay time model predicts a very low volumetric density of bursts at $z = 2.211$, whereas a power law delay time model peaks near GRB 111117A. If more sGRBs are at similarly high redshifts, but are missed due to the faintness of their hosts, a lognormal delay time model will be disfavored. Compared to a sample of sGRB hosts, GRB 111117A is more luminous than 80 per cent of a complete sample of sGRB hosts with measured luminosities. Assuming a host brightness redshift determination threshold, for between 43 and 71 per cent of sGRB hosts, we would be unable to determine a redshift should they be at a similar redshift as GRB 111117A. This could indicate that potentially, a significant fraction of sGRBs are at high z but missed due to host faintness.

Using the age of the universe at the time of explosion allows us to set constraints on the maximal separation between the engine constituents at the time of formation. We find that the maximal separation of two NSs at system formation time is $a_0 < 3.2\ R_{\odot}$, which excludes some of the formation channels with the longest timescales.

All data, code and calculations related to the paper along with the paper itself are available at `https://github.com/jselsing/GRB111117A`.

Acknowledgements. We thank Jens Hjorth and Lise Christensen for useful discussions regarding the interpretation of this event. We thank Mathieu Puech for testing the possible contribution from an older stellar population in the SED. TK acknowledges support through the Sofja Kovalevskaja Award to P. Schady. SDV is supported by the French National Research Agency (ANR) under contract ANR-16-CE31-0003 BEaPro JJ acknowledges support from NOVA and NWO-FAPESP grant for advanced instrumentation in astronomy. NRT and KW acknowledge support from STFC Consolidated Grant ST/N000757/1 CT acknowledges support from a Spanish National Research Grant of Excellence under project AYA 2014-58381-P and funding associated to a Ramón y Cajál fellowship under grant number RyC-2012-09984. AdUP acknowledges support from a Ramón y Cajal fellowship, a BBVA Foundation Grant for Researchers and Cultural Creators,and the Spanish Ministry of Economy and Competitiveness through project AYA2014-58381-P. Partly based on observations made with the Gran Telescopio Canarias (GTC). ZC acknowledges support from the Spanish research project AYA 2014-58381-P and support from Juan de la Cierva Incorporación fellowships IJCI-2014-21669. RSR acknowledges AdUP's BBVA Foundation Grant for Researchers and Cultural Creators and support from ASI (Italian Space Agency) through the Contract n. 2015-046-R.0 and from European Union Horizon 2020 Programme under the AHEAD project (grant agreement n. 654215). This research made use of Astropy, a community-developed core Python package for Astronomy (Astropy Collaboration 2013). The analysis and plotting has been achieved using the Python-based packages Matplotlib (Hunter 2007), Numpy and Scipy (van der Walt et al. 2011) along with other community-developed packages. This work made use of observations obtained with the Italian 3.6 m Telescopio Nazionale Galileo (TNG) operated on the island of La Palma by the Fundación Galileo Galilei of the INAF (Istituto Nazionale di Astrofisica) at the Spanish Observatorio del Roque de los Muchachos of the Instituto de Astrofísica de Canarias. Based on data from the GTC Archive at CAB (INTA-CSIC) and on observations obtained at the Gemini Observatory, which is operated by the Association of Universities for Research in Astronomy, Inc., under a cooperative agreement with the NSF on behalf of the Gemini partner-

ship: the National Science Foundation (United States), the National Research Council (Canada), CONICYT (Chile), Ministerio de Ciencia, Tecnología e Innovación Productiva (Argentina), and Ministério da Ciência, Tecnologia e Inovação (Brazil).

References

Antonelli, L. A., D'Avanzo, P., Perna, R., et al. 2009, A&A, 507, L45, arXiv:0911.0046v1
Arcodia, R., Campana, S., & Salvaterra, R. 2016, A&A, 590, A82, arXiv:1604.01313
Arun, K. G., Tagoshi, H., Pai, A., & Mishra, C. K. 2014, Phys. Rev. D, 90, 024060, arXiv:1403.6917
Astropy Collaboration. 2013, A&A, 558, A33, arXiv:1307.6212
Barnes, J. & Kasen, D. 2013, ApJ, 775, 18, arXiv:1303.5787
Behroozi, P. S., Ramirez-Ruiz, E., & Fryer, C. L. 2014, ApJ, 792, 123, arXiv:1401.7986
Belczynski, K., Perna, R., Bulik, T., et al. 2006, ApJ, 648, 1110
Berger, E. 2010, ApJ, 722, 1946, arXiv:1007.0003
Berger, E. 2014, ARA&A, 52, 43, arXiv:1311.2603
Bromberg, O., Nakar, E., Piran, T., & Sari, R. 2012, ApJ, 749, 110, arXiv:1111.2990
Bromberg, O., Nakar, E., Piran, T., & Sari, R. 2013, ApJ, 764, 179, arXiv:1210.0068
Bruzual, G. & Charlot, S. 2003, MNRAS, 344, 1000, arXiv:0309134
Buchner, J., Schulze, S., & Bauer, F. E. 2017, MNRAS, 464, 4545, arXiv:1610.09379
Campana, S., Thöne, C. C., de Ugarte Postigo, A., et al. 2010, MNRAS, 402, 2429, arXiv:0911.1214
Cenko, S. B. & Cucchiara, A. 2011, GRB Coord. Network, Circ. Serv. No. 12577, #1, 12577
Chabrier, G. 2003, PASP, 115, 763, arXiv:0304382
Cucchiara, A. & Cenko, S. B. 2011, GRB Coord. Network, Circ. Serv. No. 12567, #1, 12567
D'Avanzo, P., Salvaterra, R., Bernardini, M. G., et al. 2014, MNRAS, 442, 2342, arXiv:1405.5131
de Blok, W. J. G. & Walter, F. 2014, AJ, 147, 96, arXiv:1401.8158
de Ugarte Postigo, A., Castro-Tirado, A. J., Guziy, S., et al. 2006, ApJ, 648, L83, arXiv:0605516v1
de Ugarte Postigo, A., Horváth, I., Veres, P., et al. 2011, A&A, 525, A109
Della Valle, M., Chincarini, G., Panagia, N., et al. 2006, Nature, 444, 1050, arXiv:0608322
Evans, P. A., Beardmore, A. P., Page, K. L., et al. 2009, MNRAS, 397, 1177, arXiv:0812.3662
Evans, P. A., Beardmore, A. P., Page, K. L., et al. 2007, A&A, 469, 379
Fong, W. & Berger, E. 2013, ApJ, 776, 18, arXiv:1307.0819
Fong, W., Berger, E., Chornock, R., et al. 2013, ApJ, 769, 56, arXiv:1302.3221
Fox, D. B., Frail, D. A., Price, P. A., et al. 2005, Nature, 437, 845, arXiv:0510110
Fynbo, J. P. U., Watson, D., Thöne, C. C., et al. 2006, Nature, 444, 1047
Gal-Yam, A., Fox, D. B., Price, P. A., et al. 2006, Nature, 444, 1053
Gehrels, N., White, N., Barthelmy, S., et al. 2004, ApJ, 611, 1005, arXiv:0405233v1
Ghirlanda, G., Salafia, O. S., Pescalli, A., et al. 2016, A&A, 594, A84, arXiv:1607.07875
Goldoni, P., Royer, F., François, P., et al. 2006, Ground-based Airborne Instrum. Astron. Ed. by McLean, 6269, 80
Goriely, S., Bauswein, A., & Janka, H.-T. 2011, ApJ, 738, L32, arXiv:1107.0899
Hjorth, J., Sollerman, J., Gorosabel, J., et al. 2005a, ApJ, 630, L117
Hjorth, J., Watson, D., Fynbo, J. P. U., et al. 2005b, Nature, 437, 859, arXiv:0510190v1
Horne, K. 1986, PASP, 98, 609
Horváth, I., Bagoly, Z., Balázs, L. G., et al. 2010, ApJ, 713, 552, arXiv:1003.0632
Hunter, J. D. 2007, CSE, 9, 90
Ilbert, O., Arnouts, S., McCracken, H. J., et al. 2006, A&A, 457, 841, arXiv:0603217
Jakobsson, P., Hjorth, J., Fynbo, J. P. U., et al. 2004, ApJ, 617, L21, arXiv:0411036
Ji, A. P., Frebel, A., Chiti, A., & Simon, J. D. 2016, Nature, 531, 610, arXiv:1512.01558
Jin, Z.-P., Hotokezaka, K., Li, X., et al. 2016, Nat. Commun., 7, 12898, arXiv:1603.07869
Jones, A., Noll, S., Kausch, W., Szyszka, C., & Kimeswenger, S. 2013, A&A, 560, A91, arXiv:1310.7030
Kann, D. A., Klose, S., Zhang, B., et al. 2011, ApJ, 734, 96, arXiv:0804.1959
Kennicutt, R. C. 1998, ARA&A, 36, 189
Komiya, Y. & Shigeyama, T. 2016, ApJ, 830, 76, arXiv:1608.01772
Kopač, D., D'Avanzo, P., Melandri, A., et al. 2012, MNRAS, 424, 2392, arXiv:1203.1864
Kouveliotou, C., Meegan, C. A., Fishman, G. J., et al. 1993, ApJ, 413, L101, arXiv:1011.1669v3
Krühler, T., Malesani, D., Fynbo, J. P. U., et al. 2015, A&A, 581, A125, arXiv:1505.06743
Krühler, T., Malesani, D., Milvang-Jensen, B., et al. 2012, ApJ, 758, 46, arXiv:1205.4036
Krühler, T., Schady, P., Greiner, J., et al. 2011, A&A, 526, A153, arXiv:1011.1205
Leibler, C. N. & Berger, E. 2010, ApJ, 725, 1202
Levan, A. J., Tanvir, N. R., Fruchter, A. S., et al. 2006, ApJ, 648, L9
Levesque, E. M., Bloom, J. S., Butler, N. R., et al. 2010, MNRAS, 401, 963, arXiv:0907.1661
Littlejohns, O. M., Tanvir, N. R., Willingale, R., et al. 2013, MNRAS, 436, 3640, arXiv:1309.7045
Lyman, J. D., Levan, A. J., Tanvir, N. R., et al. 2017, MNRAS, 1817, stx220
Madau, P. & Dickinson, M. 2014, ARA&A, 52, 415, arXiv:1403.0007
Marchesini, D., van Dokkum, P., Quadri, R., et al. 2007, ApJ, 656, 42, arXiv:0610484
Margutti, R., Berger, E., Fong, W., et al. 2012, ApJ, 756, 63, arXiv:1205.7075v1
Margutti, R., Zaninoni, E., Bernardini, M. G., et al. 2013, MNRAS, 428, 729, arXiv:1203.1059
Milvang-Jensen, B., Fynbo, J. P. U., Malesani, D., et al. 2012, ApJ, 756, 25
Modigliani, A., Goldoni, P., Royer, F., et al. 2010, SPIE Astron. Telesc. + Instrum., 7737, 773728
Nissanke, S., Holz, D. E., Hughes, S. A., Dalal, N., & Sievers, J. L. 2010, ApJ, 725, 496, arXiv:0904.1017
Noll, S., Kausch, W., Barden, M., et al. 2012, A&A, 543, A92
Norris, J. P. & Bonnell, J. T. 2006, ApJ, 643, 266, arXiv:0601190
O'Shaughnessy, R., Belczynski, K., & Kalogera, V. 2008, ApJ, 675, 566, arXiv:0706.4139
Papovich, C., Dickinson, M., & Ferguson, H. C. 2001, ApJ, 559, 620
Planck Collaboration, Ade, P. A. R., Aghanim, N., et al. 2016, A&A, 594, A13
Postnov, K. A. & Yungelson, L. R. 2014, LRR, 17, arXiv:0701059
Richard, J., Kneib, J.-P., Ebeling, H., et al. 2011, Mon. Not. R. Astron. Soc. Lett., 414, L31, arXiv:1102.5092
Rosswog, S., Feindt, U., Korobkin, O., et al. 2017, Class. Quantum Gravity, 34, 104001, arXiv:1611.09822
Sakamoto, T., Troja, E., Aoki, K., et al. 2013, ApJ, 766, 41, arXiv:1205.6774
Schlafly, E. F. & Finkbeiner, D. P. 2011, ApJ, 737, 103, arXiv:1012.4804
Schlegel, D. J., Finkbeiner, D. P., & Davis, M. 1998, ApJ, 500, 525, arXiv:9710327
Schulze, S., Krühler, T., Leloudas, G., et al. 2016, eprint arXiv:1612.05978, arXiv:1612.05978
Starling, R. L. C., Willingale, R., Tanvir, N. R., et al. 2013, MNRAS, 431, 3159, arXiv:1303.0844
Tanvir, N. R., Levan, A. J., Fruchter, A. S., et al. 2013, Nature, 500, 547, arXiv:1306.4971
Thöne, C. C., Campana, S., Lazzati, D., et al. 2011, MNRAS, 414, 479, arXiv:1101.3488
Tunnicliffe, R. L., Levan, A. J., Tanvir, N. R., et al. 2014, MNRAS, 437, 1495, arXiv:1402.0766v1
van de Voort, F., Quataert, E., Hopkins, P. F., Kere, D., & Faucher-Giguere, C.-A. 2014, MNRAS, 447, 140, arXiv:1407.7039
van der Walt, S., Colbert, S. C., & Varoquaux, G. 2011, CSE, 13, 22
Vernet, J., Dekker, H., D'Odorico, S., et al. 2011, A&A, 536, A105, arXiv:1110.1944
Wallner, A., Faestermann, T., Feige, J., et al. 2015, Nat. Commun., 6, 5956, arXiv:1509.08054
Wanderman, D. & Piran, T. 2015, MNRAS, 448, 3026, arXiv:1405.5878
Willingale, R., Starling, R. L. C., Beardmore, A. P., Tanvir, N. R., & O'Brien, P. T. 2013, MNRAS, 431, 394, arXiv:1303.0843
Yang, B., Jin, Z.-P., Li, X., et al. 2015, Nat. Commun., 6, 7323, arXiv:1503.07761
Zhang, B., Zhang, B.-B., Virgili, F. J., et al. 2009, ApJ, 703, 1696, arXiv:0902.2419